ELECTRICAL AND THERMOSTRUCTURAL ANALYSES OF POTTED HIGH-VOLTAGE ELECTRONIC DEVICES

Donna K. Archipley-Smith
Henry H. Fong

PDA Engineering
Santa Ana, California 92705

INTRODUCTION

The use of elastomeric potting compounds is common in high-voltage electronic devices, for high-voltage standoff, heat transfer, and vibration isolation purposes. Electrical and/or mechanical breakdown often occur in such devices due to arcing, cracks and flaws, and stress concentration due to severe constraint conditions aggravated by the nearly incompressible behavior of typical potting materials. The finite-element analysis of such potted devices is complex, and is often hampered by an inadequate material property base. This paper presents the results of a nine-month 1981 study aimed at understanding the electrical and thermostructural behavior of a potted gun assembly of a traveling wave tube (TWT) used in a communications satellite.

A TWT is an electronic device which operates in vacuum conditions and consists of an electron gun, a slow-wave circuit, and a collector (Figure 1). It can be used in electronic countermeasure, radar, and spacecraft communication systems. It is usually less than a few feet in length, but has a complex shape which is both difficult to package and to analyze. The gun "fires" electrons down the circuit (which accelerates the beam) and the collector dissipates the heat energy. This study addressed the electrical, heat transfer, stress, and dynamic behavior of one such TWT; however, only the gun electrical and stress results are included in this paper. The electrical analysis discusses the implementation of the methodology using the heat transfer option in the MSC/NASTRAN code, modeling considerations in an electrical problem, and results for an axisymmetric gun model as well as a localized three-dimensional model near a solder ball. The thermostructural analysis describes the state-of-the-art in finite element analysis of nearly incompressible materials, gun axisymmetric model stresses, and the performance of the QUAD4 element in a plane strain test case.

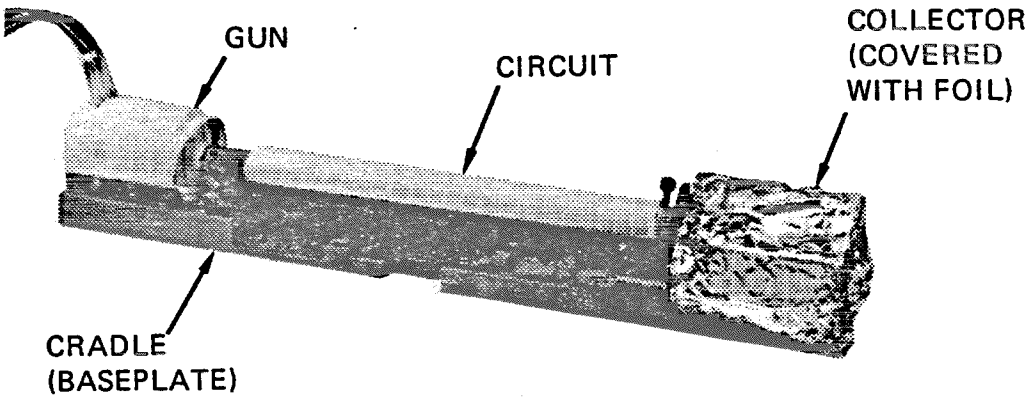

(NOTE: TWT COVER NOT SHOWN)

TRAVELING WAVE TUBE

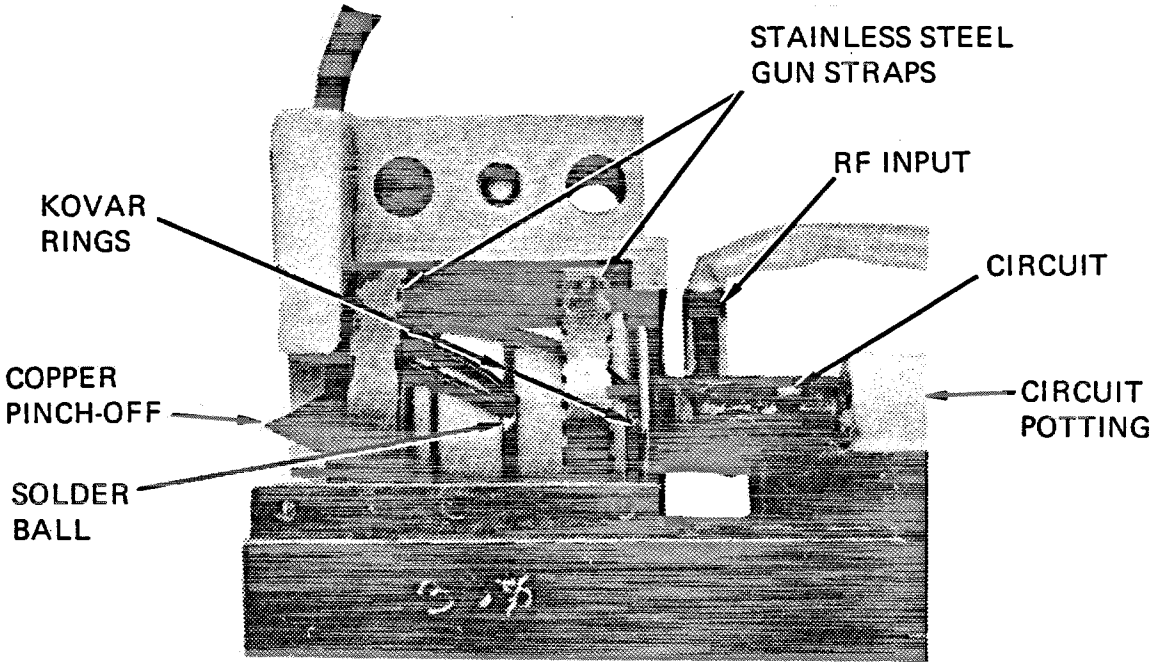

SIDE VIEW OF UNPOTTED GUN SHOWING STRAPS, WIRES, AND TYPICAL SOLDER BALL

Figure 1. Typical Traveling Wave Tube and View of Unpotted Gun

ELECTRICAL ANALYSIS

Background

The effective operation of a high voltage device, such as a TWT, is dependent on its ability to maintain potential differences across different dielectric media. If, at any time, design-induced electrical stresses in the device exceed the dielectric withstanding strength of a material, electrical breakdown will occur.

Normally, electrical stresses in a TWT are not sufficient to cause this type of breakdown across a solid dielectric material. However, if a dielectric material, for some reason, possesses discontinuities (such as voids, cracks, or surface delamination), a partial breakdown can occur at a much lower electrical stress level. In time, a partial breakdown, if the TWT is further stressed, will ultimately lead to a complete electrical failure.

Past studies have indicated that the most likely mode of electrical failure in this TWT design is a growth in potting material discontinuities with time due to mechanical stresses, accompanied by a growth in partial discharges and inducing a complete electrical failure. It was the objective of this analysis effort to assure that combined mechanical and electrical stress levels were insufficient to induce such a failure mechanism.

Methodology

- Electrical/Thermal Field Analogy

In past electrical analyses of TWTs, one of several finite difference codes (e.g., Herrmannsfeldt) has been utilized. For the first time, this analysis effort employed the finite element method (as implemented in the MSC/NASTRAN code). This method offered two important advantages: improved accuracy in analytical results, and modeling consistency among the electrical/mechanical/thermal/dynamic analyses.

Although an electrostatic field analysis capability is not explicitly available in MSC/NASTRAN, the heat transfer option can be used to calculate electric fields, voltages, and electrical stresses [1,2,3]. The initiation and propagation of electrostatic fields is governed by one of Maxwell's four electromagnetic equations:

$$\nabla \cdot \varepsilon \vec{E} = \rho \qquad (1)$$

where $\nabla = \underline{i}\,\frac{\partial}{\partial x} + \underline{j}\,\frac{\partial}{\partial y} + \underline{k}\,\frac{\partial}{\partial z}$, ϵ is permittivity, E is electric field, and ρ is volumetric charge density. The relationship between potential and the electrical field is defined as

$$\vec{E} = -\nabla V \tag{2}$$

The electrical diffusion equation is then obtained by substituting (2) into (1):

$$\nabla \cdot \epsilon \nabla V + \rho = 0 \tag{3}$$

The electrical diffusion equation is thus analogous to the heat transfer equation

$$\nabla \cdot K \nabla T + \dot{q} = \rho c \left(\frac{\partial T}{\partial t}\right) \tag{4}$$

where K is thermal conductivity, T is temperature, $\dot{q}$ is internal heat generation, and ρc is heat capacity per unit volume. A summary of thermal/electrical parameter relationships is shown in Figure 2.

- STATIC ELECTRICAL/THERMAL FIELD EQUATIONS

$\nabla \cdot \epsilon \vec{E} = \rho$	GAUSS' LAW (DIFFERENTIAL FORM)
$\vec{E} = -\nabla V$	ELECTRIC POTENTIAL
$\nabla \cdot \epsilon \nabla V + \rho = 0$	ELECTRICAL DIFFUSION EQUATION
$\nabla \cdot K \nabla T + \dot{q} = \rho c \left(\frac{\partial T}{\partial t}\right)$	ANALOGOUS HEAT DIFFUSION EQUATION USED IN HEAT TRANSFER SOLUTION

- ELECTRICAL – THERMAL FIELD COMPARISONS

THERMAL INPUT PARAMETERS		ELECTRICAL INPUT PARAMETERS	
TEMPERATURE	T	POTENTIAL	V
CONDUCTIVITY	K	PERMITTIVITY	ϵ
TEMPERATURE GRADIENT	∇T	ELECTRIC FIELD	$\vec{E}$
HEAT FLUX	$-K\nabla T$	ELECTRIC DISPLACEMENT	$\vec{D}$
INTERNAL HEAT GENERATION	$\dot{q}$	CHARGE DENSITY	ρ

Figure 2. Electrical Stress Analysis of a Static Field

- MSC/NASTRAN Implementation

By replacing NASTRAN heat transfer inputs and outputs with analogous electric field parameters, this solution technique was utilized to predict electrical stresses. Code implementation included input stream development, solution run, and results formulation (Figure 3).

The definition of an electrostatic problem includes primarily setting boundary conditions which reflect applied voltages (and any initial surface charges) and describing the relative behavior of materials under the influence of an electric field.

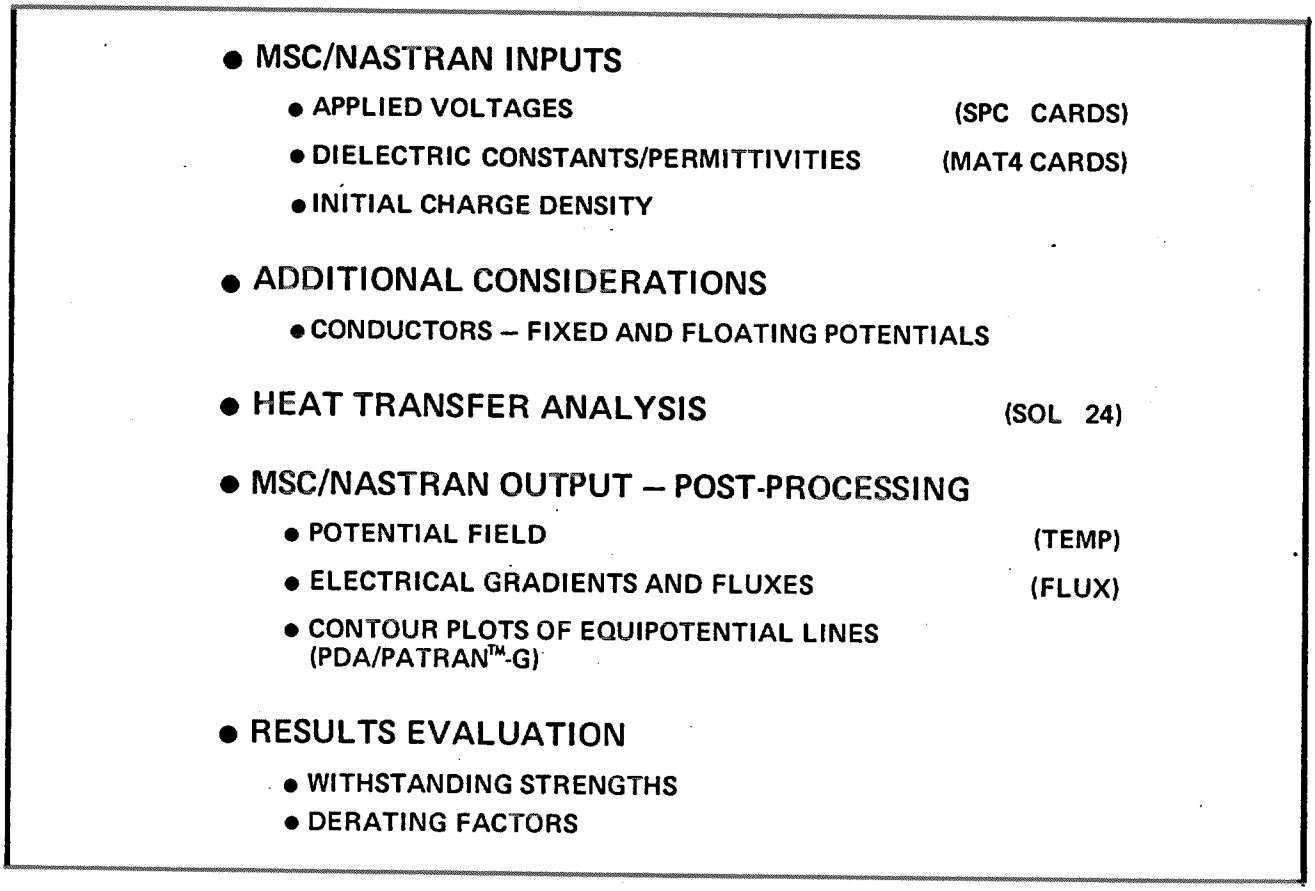

Figure 3. Electrical Stress Analysis Methodology Implemented in MSC/NASTRAN

The material property incorporated in the electric diffusion equation, which characterizes dielectric material behavior in a static field, is a permittivity value (or dielectric constant). This value is a relative measure of the ability of a dielectric material to store energy. In addition to materials that are in the insulating (or dielectric) classification, there are often materials involved which fall into the category of conductors. Since conductors respond differently than dielectrics and are not characterized by a permittivity value, they must either be forced into the form of a dielectric, or treated in a different manner. In this case, there were conductors present which were at both fixed and floating potentials. Fixed-potential conductors were replaced with boundary condition constraints. Values of floating potentials were calculated employing classical equations governing multiple dielectric interfaces, along with geometric considerations. In turn, these potentials were also applied as constraints on conducting surfaces. Boundary condition constraints reflecting high voltage and ground potential operating conditions of the TWT were applied to complete definition of the problem.

Rigid format SOL 24 (Heat Transfer) was utilized in the analysis with two primary outputs requested: the voltage field (giving potential values at each grid point), and electrical gradients and fluxes (determining electrical stresses).

- Results Evaluation

Correlation of results consisted of evaluating predicted electrical stresses against the ultimate withstanding strength of the appropriate dielectric material. Due to combined electrical/mechanical time-dependent material degradation, and the possibility of partial discharging, the ultimate withstanding strength of each material is usually assigned a derating factor. Once derated, all predicted stresses must not exceed material strengths in order to assure a safe design.

Gun Axisymmetric Electrical Model

Because mechanical and electrical stresses combine to cause detrimental effects on the potting material, it was important to superpose these values on identical analytical models. This enables regions of simultaneously high electrical-mechanical stresses to be identified as potential problem areas.

For this purpose, a 2-D axisymmetric gun model was generated using PDA/PATRAN^{TM}-G for both the electrical and mechanical analyses. The completed model encompassed the entire gun region, and included: the internal electron beam structures (anode, heater-cathode, focus electrode, and support structures), the internal vacuum region, the entire gun body (ceramic rings, conducting support rings, Kovar weld cup, copper pinch-off, and electrical connection tabs), the surrounding potting layer, and the two gun body support straps. The completed model reflected a moderately fine mesh which consisted of 462 TRAPRG and TRIARG NASTRAN elements.

The electrical analysis of this model accounted for the worst-case operating conditions of the tube. All internal structures were held at high voltage (4000 volts), the gun support straps and outer gun cover were grounded, and all floating conductor voltages were assigned calculated values. The results of this electrical analysis (Figure 4) revealed a maximum stress in the potting material of 50.9 volts/mil, located around the electrical connection tab of the anode.

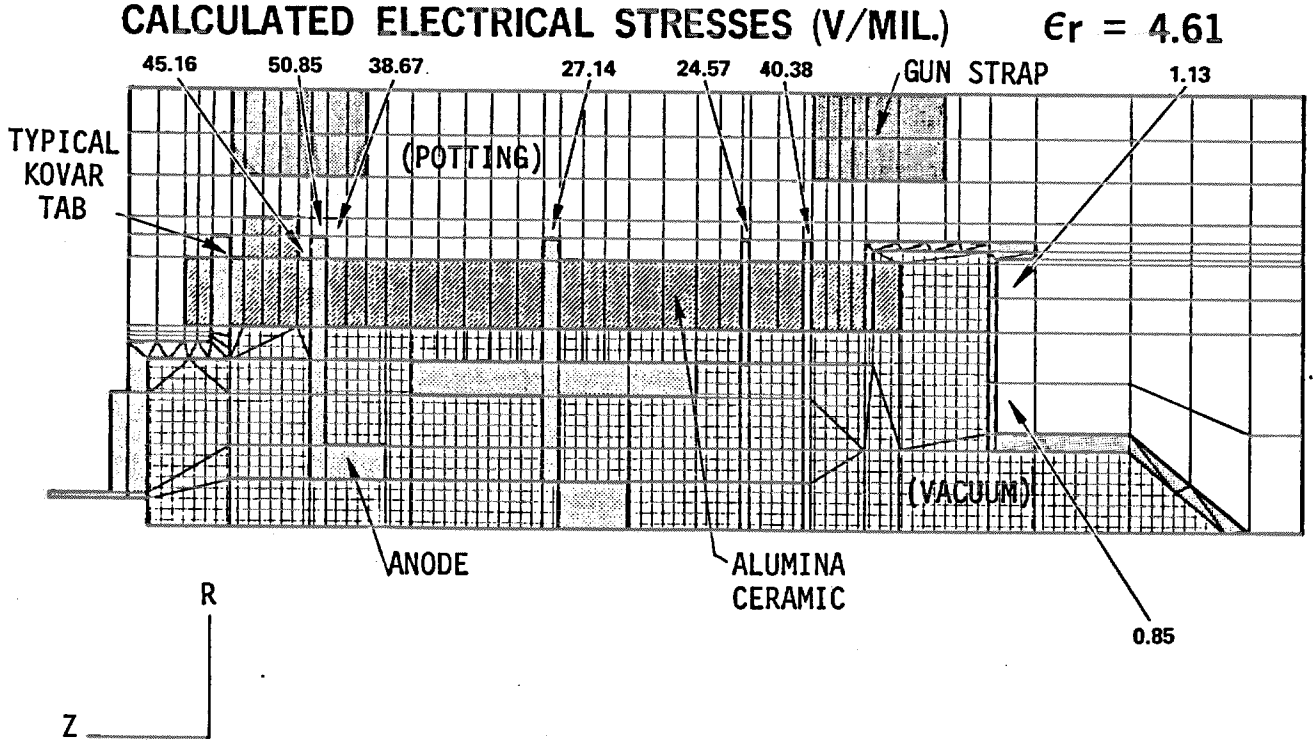

Figure 4. Axisymmetric Gun Electrical Analysis

Areas with protrusions, material discontinuities, or sharp corners will experience concentrated levels of electrical stress. Because this model was axisymmetric, the effect of sharp corners on electrical connection tabs was not accounted for in the calculation of electrical stresses. In addition, this model lacked the representation of solder balls, placed above the connection tabs in the manufacturing process.

Gun 3-D Tab Model

In order to further investigate gun electrical stresses, a refined 3-D model was generated. This model was limited to a small area around the anode electrical connection tab. A 3-D representation was deemed necessary to accurately analyze local stresses affected by sharp corners and a solder ball. This model extended 0.335-inch in the axial direction, 0.275-inch in the radial direction, 30° in the circumferential direction, and consisted of 113 8-noded HEXA solid elements. Structures included in the model were: the anode connection tab, the solder ball, a section of the anode support ring, the surrounding potting region, and small sections of ceramic gun body rings.

Imposed boundary conditions on this model were identical to those applied on the 2-D axisymmetric gun model. Any additional unknown boundary points were calculated using data obtained from the 2-D gun model.

Results on the refined model predicted a maximum electrical stress of 60.2 volts/mil. The location of this element and other high stressed elements was directly above the top of the solder ball. Around the sides of the solder ball, element stresses averaged 30 to 40 volts/mil (Figure 5). Utilizing a 4-to-1 derating factor (justified by having a detailed finite element analysis) for the ultimate withstanding strength of the Adiprene potting, the maximum allowable stress level is 100 volts/mil [4]. With the thorough analytical study completed on this region, electrical stress levels were, therefore, considered safe.

THERMOSTRUCTURAL ANALYSIS

Recent progress has been made in the thermal stress analysis of potted components in TWTs. First, some background information will be given: TWT finite element analysis accomplishments in the past two years; practical considerations in the analysis of near incompressibility problems and comments on the current ability of some commercial FEM codes to handle this class of problems; and material properties of the Adiprene L-100 potting studied.

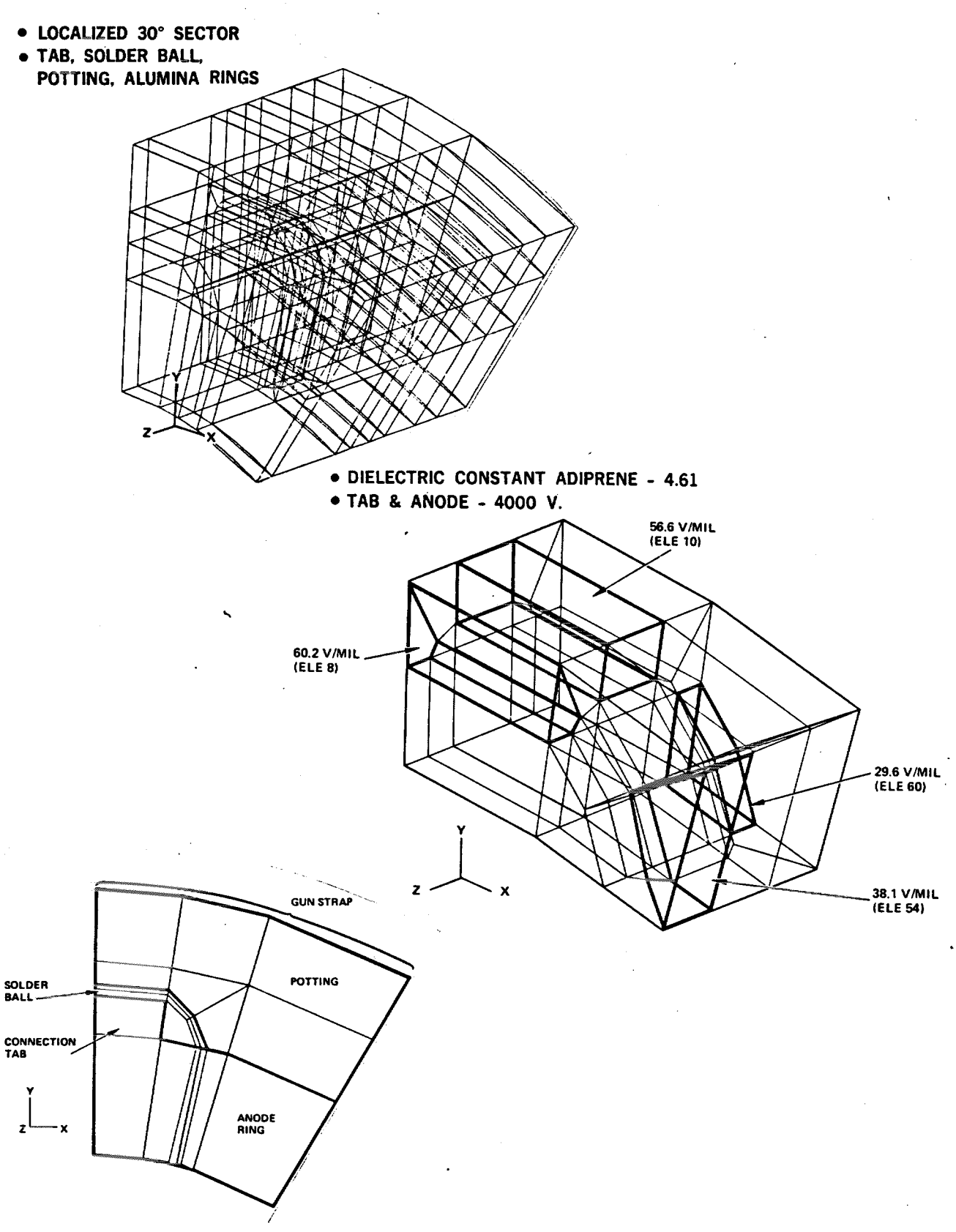

Figure 5. 3-D Gun Tab and Solder Ball Model

Second, the same gun axisymmetric model developed for the electrical analysis was utilized for the thermal stress analysis, showing the locations and magnitudes of peak electrical/mechanical stresses. And third, a near incompressibility study was conducted comparing the MSC/NASTRAN QUAD4 and PDA/SAAS quadrilateral elements in a plane-strain model of the potting near a Teflon-coated copper wire.

Background

- TWT Finite Element Analyses

In late 1979, D. J. Chang of The Aerospace Corporation was the first to conduct finite-element stress analyses of severely constrained potted regions in a TWT collector. The 2-D SAAS III code was used, and he found very high Adiprene potting tensile stresses during cooldown from the 85°C cure temperature to a cold (-30°C) spacecraft operational extreme. At about the same time, Fong and Hamel [5,6] presented thermal/structural finite element results of various TWTs and components. The MSC/NASTRAN and ANSYS codes were used. One ANSYS 3-D superelement, coupled thermal/structural analytical study produced a correlation of ±5 percent with measured thermocouple data and ±16 percent with strain gage data. In 1980, Vichnin and Fong [7] applied the MARC, MSC/NASTRAN, and SAAS III codes to analyze potting stresses in the collector and gun regions of the same TWT analyzed by Chang. A 850-element SAAS plane-strain model (using 4-node Wilson solid-of-revolution elements) at a Poisson's ratio ν of 0.499 was found to predict displacements and stresses 15 percent lower than an equivalent MARC model of 90 elements (8-node isoparametrics, with Herrmann pressure variable at each corner node and $\nu = 0.5$). Design improvements were recommended to alleviate the high potting stresses. In axisymmetric analyses using the NASTRAN TRAPRG element, NASTRAN-predicted stresses were within 7 percent of a similar but coarser MARC model (using 8-node isoparametric elements and 3 x 3 Gaussian integration) at $\nu = 0.48$. A viscoelastic MARC stress analysis, using a "thermo-rheologically simple" model and limited stress relaxation data, predicted a 25 percent stress reduction after 13.3 minutes. The same potting stress analysis methodology was applied by Vichnin (using MSC/NASTRAN) to analyze a General Electric high voltage power supply module. Peak stress locations coincided with crack locations observed in tests. However, the peak stress predicted was a fraction of the static strength, leading to the hypothesis that a slow crack growth phenomenon exists in the potting which ultimately results in potting failure after many thermal cycles.

• Finite Element Analysis of Near Incompressibility Problems

If a region of potting material is fully constrained, the closed-form solution for the thermal stress (which is hydrostatic, or equal in all directions), σ, is:

$$\sigma = - \frac{E\alpha\Delta T}{1-2\nu} = -3\ K\alpha\Delta T$$

where E is Young's modulus, α is coefficient of thermal expansion, ΔT is the temperature change, ν is Poisson's ratio, and K is bulk modulus. For a negative ΔT, σ is tensile. When ν is 0.5 (incompressible), σ is thus infinite. Therefore, the closeness of ν to 0.5 and the actual degree of constraint existing in a potted configuration (best estimated by a finite element model and analysis) are of paramount importance in determining the magnitude of the thermal stress.

When the material response is incompressible, the solution to a problem cannot be obtained in terms of the displacement history only, since a purely hydrostatic pressure may be added without changing the displacements. The nearly incompressible case (that is, the bulk modulus is very much larger than the shear modulus) exhibits behavior approaching this limit, in that a very small change in displacement produces extremely large changes in pressure so that a purely displacement-based solution (like in most finite element codes) is too sensitive to be useful numerically. For example, round-off error on the computer may cause a method to fail.

For a linear elasticity problem, the shear modulus G and the bulk modulus K may be written in terms of E and ν:

$$G = \frac{E}{2(1+\nu)} \qquad K = \frac{E}{3(1-2\nu)}$$

In the tabulation below, the quantities G/E and K/E are shown as ν is varied from 0.49 to 0.5. The bulk modulus is very sensitive to small changes of ν in this range, but the shear modulus is not.

ν	G/E	K/E
0.4900	0.3356	16.7
0.4950	0.3344	33.3
0.4990	0.3336	167
0.4995	0.3334	333
0.4999	0.3334	1667
0.5000	0.3333	∞

This tabulation suggests that a valid method to obtain ν is to measure K and E. A dilatometric test determines bulk modulus from the volume change under hydrostatic stresses, that is, $K = -\Delta V/V$. Once K and E are determined, ν can be determined from the equation:

$$\nu = 1/2 \left(1 - \frac{E}{3K}\right) .$$

The solution of incompressible and nearly incompressible problems using finite element techniques is currently an active research topic [8-15], and the elasticity problem has parallels in plasticity, metal forming processes, incompressible fluid flow, and soil plasticity problems. In 1965, Herrmann [8] was the first to solve the incompressibility problem by using a mixed formulation based on variational principles, whereby a pressure-like variable was introduced as an extra nodal unknown to impose a constant-volume constraint. In 1974, Nagtegaal, et al. [9] demonstrated that, as in plasticity problems, for any finite element the ratio of "degrees of freedom to constraints" was important in evaluating its suitability in nearly incompressible analysis. The concept of "mesh locking" was thus introduced; an element cannot be "over-constrained" if convergence is desired with mesh refinement. Malkus and Hughes have successfully applied penalty function and selective integration techniques [10-12]. They advocated using reduced integration on the dilatational part of the strain energy, and emphasized the importance of achieving the correct rank of the matrices.

The best recent overview paper is by Webster [13], who classified these finite element approaches into three types: (1) mixed field methods (e.g., Herrmann reformulation of variational principle and the use of a mean pressure variable, S. Key's orthotropic extension, and Scharnhorst and Pian's hybrid stress method); (2) reduced integration methods (e.g., Hughes and Malkus' selective integration technique, also known as the "penalty function" method); and (3) constraint methods (e.g., Argyris and his colleagues imposing global constraints via Lagrange multipliers to enforce "isochoric" or "constant-volume" strain states, and Needleman and Shih's two-pass method using an approximate stress-field calculation from a normal compressible solution to impose the isochoric constraints on a second solution). In addition to mesh-locking concerns, the latest research in this area has revolved around "pressure checkerboarding" effects on the validity of analytical stations. No one method has emerged to be the correct solution!

The suitability of commercial FEM packages [16] to handle full/near incompressibility problems is not well-known. MSC/NASTRAN [13,15] is adequate for predicting stresses to $\nu = 0.45$ in 3D problems, using its 20-node isoparametric solid element named HEX20. ABAQUS, a new second-generation nonlinear general purpose code developed by Hibbitt, Karlsson, and Sorensen, Inc., features hybrid stress elements based on an augmented variational principle. It can handle the $\nu = 0.5$ case. The incompressible elements allow a continuous displacement field and an independent pressure variation for each element. Its incompressible elements include 4-node and 8-node quadrilateral elements, for constant-pressure and linear-pressure variations, as well as their 3D counterparts, 8-node and 20-node hexahedra. ADINA, an advanced version of NONSAP developed by Professor K. J. Bathe of M.I.T., uses a concept of "approximate constraints" and a penalty function technique to be the basis of its 2D and 3D curved incompressible elements. However, its nonlinear elastic capability for Mooney-Rivlin type rubber materials undergoing large deformations is currently restricted to a plane stress problem. MARC, the oldest of the nonlinear general purpose codes, contains within its element library "Herrmann elements" to handle the $\nu = 0.5$ case, with use of a Herrmann pressure variable (an additional degree of freedom at each corner node) and a concomitant increase in cost. Reduced integration options are offered to the user. The nonlinear elastic and viscoelastic capabilities in MARC are the most extensive offered in any general purpose code.

- Material Properties of Adiprene L-100 Potting

The potting compound studied was DuPont Adiprene L-100 resin, filled with fine alumina powder to 70 percent by weight, with a Silane Z6040 additive to promote adhesion. It was cured at 52°C. Mold release was applied to the TWT gun strap surfaces to avoid a constrained situation. Typical averaged properties for this potting are:

Property	-22°C	21°C
Young's modulus E (psi)	2,818	2,196
Ultimate tensile strength σ_{tu} (psi)	2,183	654
Elongation e (%)	273	114
Poisson's ratio, stress-strain curves and volume change (from gas dilatometer test)	(See Figure 6)	
Coefficient of thermal expansion α (10^{-5} in./in./°C)	17.0	17.5

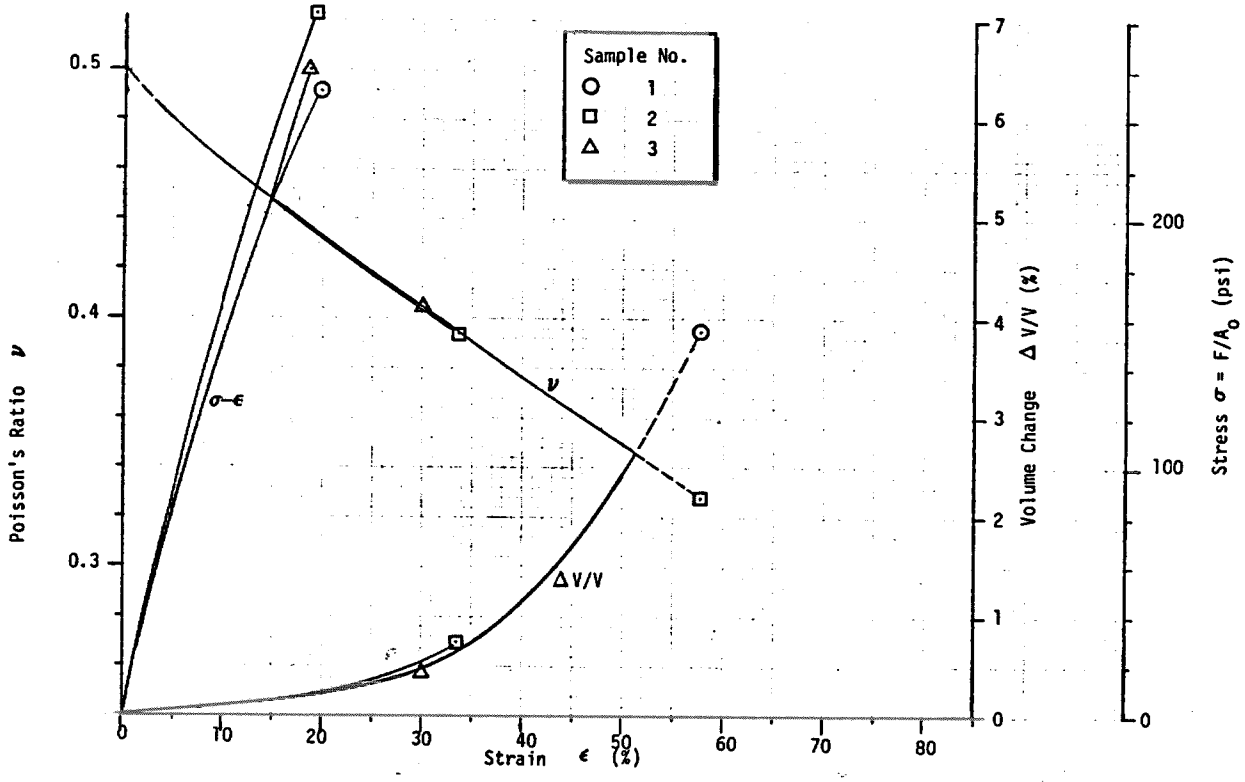

Figure 6. Poisson's Ratio, Stress-Strain, and Volume Change Data for 70%-filled Adiprene (cured at 52°C, with Silane), at 21°C and Crosshead Speed of 1.6 in./min.

Gun Axisymmetric Stress Analysis

Axisymmetric models of the gun were developed using the NASTRAN TRAPRG (trapezoidal) and TRIARG (triangular) ring elements. The TRAPRG element is quite restrictive in modeling versatility, since the user is required to have two sides of the quadrilateral element parallel and these sides must be perpendicular to the Z-axis of symmetry [17]. Its node numbering scheme also requires the first node to be at the lowest Z-value. Model generation was facilitated by use of the PDA/PATRAN™-G color interactive graphics preprocessor.

Models 1 and 2 included elements to model the metallic and alumina ceramic components of the gun body, in addition to the potting elements. These models also were used to investigate various ways to simulate the mold-released gun strap surfaces. We then realized that a modeling simplification can be made to take advantage of the fact that the non-potting materials were typically three orders of magnitude stiffer than the potting, while the latter had a much higher coefficient of thermal expansion.

This revelation resulted in the simplification to a "potting-only" model, where non-potting materials such as metals and ceramic were eliminated from the model and the bonded edges were assumed fixed. Verification of this modeling assumption was obtained when the "potting only" Model 3 gave almost identical stresses to the previous full gun model. This simplification saved about 25 percent computer time. Figure 7 shows this axisymmetric "potting only" gun model, deformed geometry, and some peak stress locations. (Model 3A was a slight variation in the strap boundary conditions; it gave about the same stresses as Model 3.) The cooldown peak potting tensile stress of 390 psi was deemed very low compared to a potting static tensile strength of 2183 psi, and the conclusion was that gun potting thermal stresses would not be a problem. This conclusion, of course, was based on a linear elastic static analysis, and did not include complex and nonlinear effects such as viscoelasticity, cracks/debonds, thermal cycling, and non-homogeneity of the potting due to the presence of the fine alumina particles.

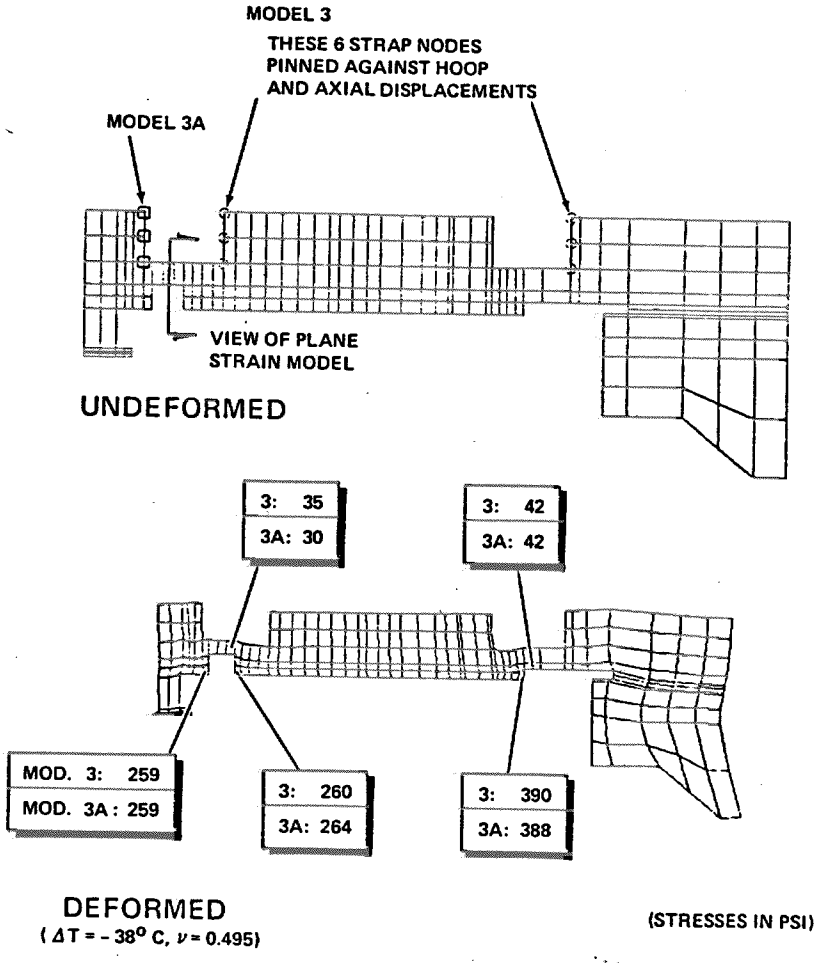

Figure 7. Gun Axisymmetric "Potting Only" Model - Deformed Geometry and Peak Potting Stresses and Locations

Figure 8 is a superposed plot of peak gun electrical and mechanical stresses. The peak voltage of 50.9 volts/mil occurred in Element 176, while the peak mechanical stress of 390 psi was in Element 276. Due to possible time-dependent synergistic effects between electrical and mechanical stresses, failure can conceivably occur at a location where neither is a maximum. A recommendation was, therefore, made to derive a combined electrical/mechanical failure criterion, which accounts for time- and temperature-dependent effects and can be substantiated by test data. (The U.S. Air Force is sponsoring just such a study over the next three years.)

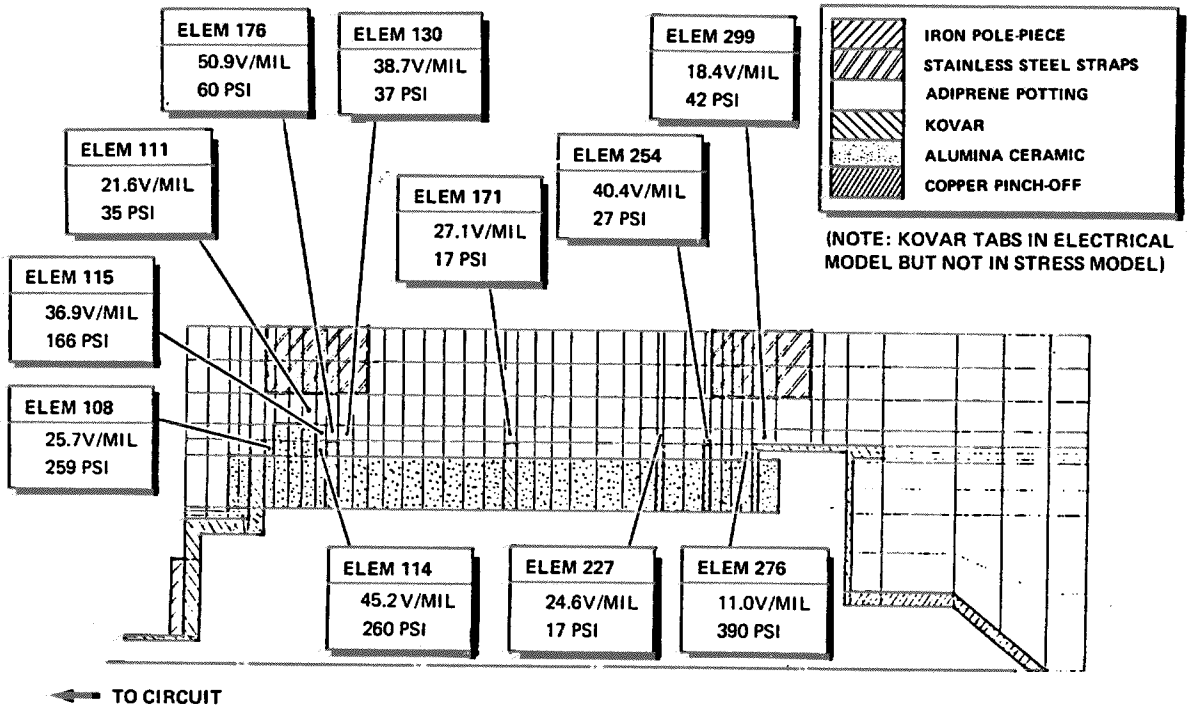

Figure 8. Superposition of Voltages and Thermomechanical Stresses in Gun Axisymmetric Model

Near Incompressibility Study—MSC/NASTRAN Versus PDA/SAAS

The original motivation for this parametric study was the question: what is the stress concentration in the potting due to a wire? Several such Teflon-coated copper wires exist in the gun (Figure 1). We decided to study the constrained area between a strap and the gun body ceramic, using a plane strain model. PATRAN was used to generate a 30° sector model, and the identical mesh was analyzed using both MSC/NASTRAN and PDA/SAAS in a near imcompressibility situation. (Note that although the mesh is identical, the SAAS model

is slightly less stiff than the NASTRAN model because of the existence of a middle node in each element.)

- The PDA/SAAS Four-triangle Quadrilateral Element

SAAS III [18] is an efficient special-purpose 2D code for plane strain, plane stress, and axisymmetric stress analyses of orthotropic solids. It has been successfully used at many companies in the past decade. Figure 9 shows the basic SAAS element, which is a quadrilateral comprised of four non-overlapping triangular elements. Recently, we have been investigating the performance of this element in several near incompressibility studies. The following is a brief summary of our findings.

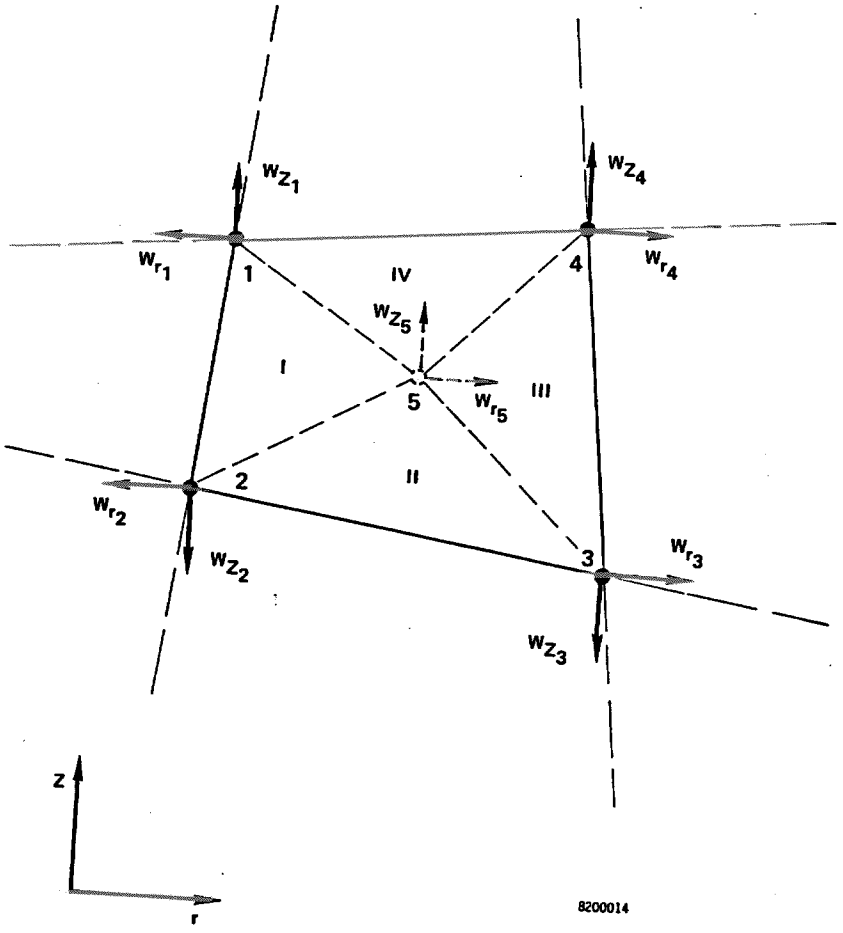

Figure 9. SAAS Quadrilateral Element in a Two-Dimensional Continuum

E. L. Wilson originally developed this element in 1965. The existence of the middle node means there are a total of ten degrees of freedom for the element, which are "statically condensated" to eight prior to solution. Inclusion of this middle node, as it turned out, gave the quadrilateral more flexibility and was precisely the feature which enabled the element to be free from "mesh locking" phenomena in near incompressibility problems. Nagtegaal, et al. [9] demonstrated this in 1974, and proved the reason for its success. They conceived the idea of counting the ratio of "the degrees of freedom divided by the number of incompressibility constraints available" for an element as a measure of its performance in near incompressibility situations. In mesh refinement, the idea is to have the resultant degrees of freedom increase faster than the constraints. Hence, a Nagtegaal count of greater than one guarantees an element will converge with mesh refinement, a count of one means a marginal case, and a count of less than one implies "mesh locking" (the element is inherently constrained such that no amount of mesh refinement will produce convergence).

Nagtegaal proved in the paper that, for the case of this four-triangle quadrilateral, the count is 4/3, which means the element converges with mesh refinement and will not lock. We have checked this element against a Herrmann test problem [8], which features a thick-walled rubber cylinder constrained by a metal shell and under internal pressure. In both axisymmetric and plane strain solutions to this problem at ν of 0.4995, we found the SAAS element to give displacements and stresses which correlated well with Herrmann's "exact" analytical solution and his finite-element solution. In addition, we have also attained success in the 0.499+ range comparing the SAAS approach with a MARC (ν = 0.5) solution, and with another special-purpose code named HHERM (ν = 0.5) in a frozen soil near incompressibility study. Therefore, in such problems, the SAAS four-triangle quadrilateral element has been demonstrated to have many merits, such as economy and sufficiently adequate precision in most cases.

- 30° Sector Plane Strain Model of Potting Near Copper Wire

The constrained potting between the gun strap and alumina ring was modeled using a 30° sector plane-strain model (Figure 10). The potting radial thickness was 75 mils. A typical wire cross-section consisted of a total diameter of 65 mils, which contained a copper wire diameter of 25 mils surrounded by 20 mils of Teflon insulation. The potting mesh near the wire was

purposely refined. A 30° sector was assumed to be sufficient to study far-field effects. Three model boundary condition variations were studied. Model 4A was the most realistic; it allowed the copper wire and Teflon wrap to contract radially. Model 4B was like an infinitely stiff wire, restrained against axial (Z) and radial motion. Model 4C was the other extreme. It had no copper wire, the Teflon and potting could move radially, and the wire was unconstrained axially. Model 4A was analyzed using both MSC/NASTRAN and PDA/SAAS, for a cooldown case of $\Delta T = -38°C$, and $\nu = 0.475, 0.485, 0.495, 0.499$. Displacement and stress correlation results will now be discussed. (Note that in Figure 10, the identical stresses in Element 273 for Cases 4A, 4B, and 4C signify that the 30° sector was adequately wide).

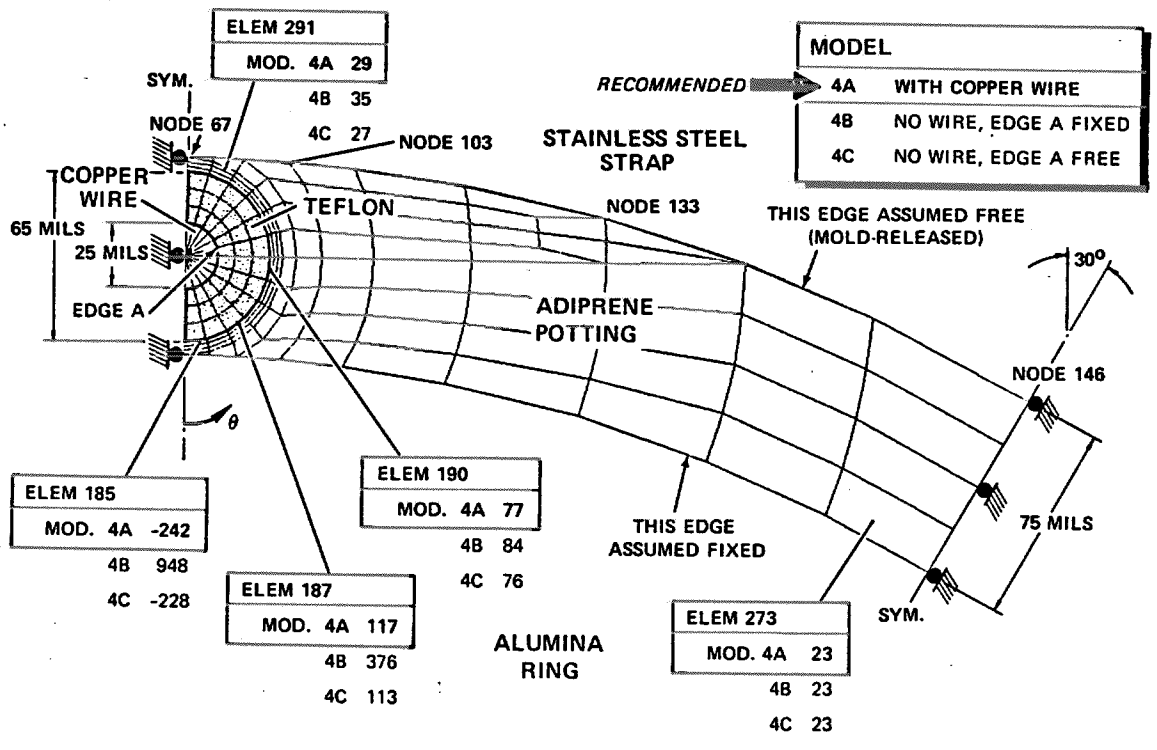

Figure 10. 30° Sector Plane Strain Model of Potting Near Copper Wire, Maximum Principal Stresses (psi) in Potting for $\Delta T = -38°C$ and $\nu = 0.495$

- Displacement Correlation

The good correlation between vertical displacement predictions from MSC/NASTRAN and SAAS at four outer edge circumferential potting nodes is summarized in the following table:

Poisson's Ratio	Analysis Code	Vertical Displacement (10^{-3} in.)			
		Node 67	Node 103	Node 133	Node 146
0.475	MSC/NASTRAN	-.455	-.923	-1.195	-1.215
	PDA/SAAS	-.455	-.913	-1.195	-1.214
0.485	MSC/NASTRAN	-.453	-.947	-1.225	-1.245
	PDA/SAAS	-.455	-.932	-1.225	-1.242
0.495	MSC/NASTRAN	-.445	-.973	-1.291	-1.248
	PDA/SAAS	-.451	-.950	-1.258	-1.270
0.499	MSC/NASTRAN	-.443	-.972	-1.215	-1.367
	PDA/SAAS	-.445	-.954	-1.267	-1.279
0.4995	MSC/NASTRAN	-.451	-.967	-1.193	-1.397
	PDA/SAAS	-.443	-.954	-1.267	-1.278
0.4999	MSC/NASTRAN	(not analyzed)			
	PDA/SAAS	-.442	-.958	-1.267	-1.270

- Stress Correlation

Figure 11 shows the maximum principal stress distributions in the first row of twelve elements around the wire Teflon periphery (from the bottom to the top) for the four Poisson's ratios studied. The predicted stress correlation between MSC/NASTRAN and PDA/SAAS is excellent at ν = 0.475 and 0.485, fair at ν = 0.495, and poor at ν = 0.499. A typical SAAS run costs half as much as a corresponding NASTRAN run.

Figure 12 is a summary of maximum principal stress and strain versus Poisson's ratio. SAAS results are also shown for ν = 0.4995 and 0.4999. The QUAD4 element (used in plane strain) starts to diverge at $\nu > 0.49$. It turns out the Teflon wrap acts as an important transition layer and the anticipated stress concentration did not materialize. The maximum principal stresses predicted are lower than the measured potting tensile strength. The study further demonstrated the reliability of the PDA/SAAS four-triangle quadrilateral element in near incompressibility studies. The MSC/NASTRAN QUAD4 (used in plane strain) should not be used for stress predictions above ν = 0.49, although as expected, its displacement predictions are reasonably accurate at Poisson's ratios higher than this value.

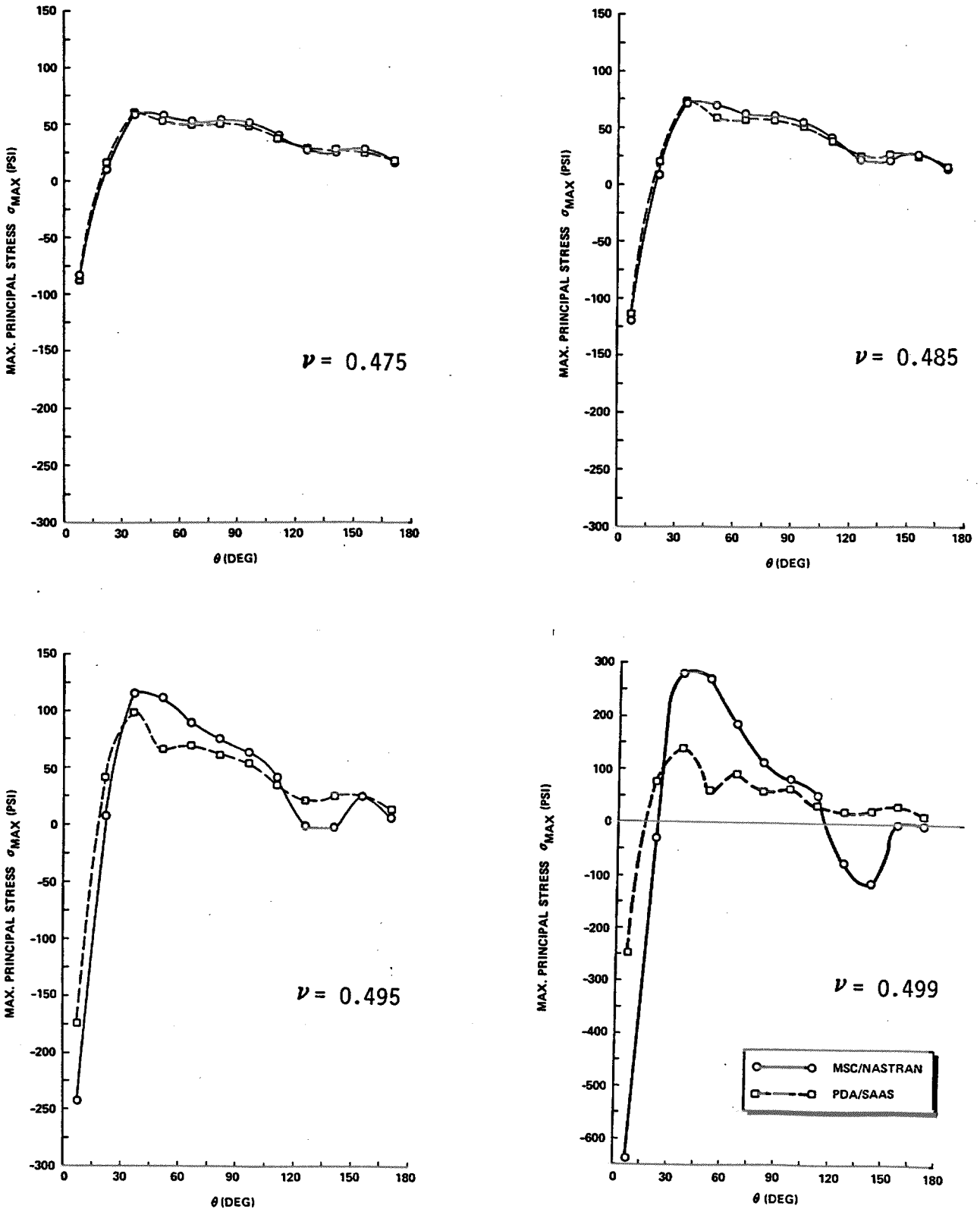

Figure 11. Plane Strain Model of Potting Near Cooper Wire— σ_{max} Comparison of MSC/NASTRAN Versus PDA/SAAS at ν = 0.475, 0.485, 0.495, 0.499 (ΔT = -38°C)

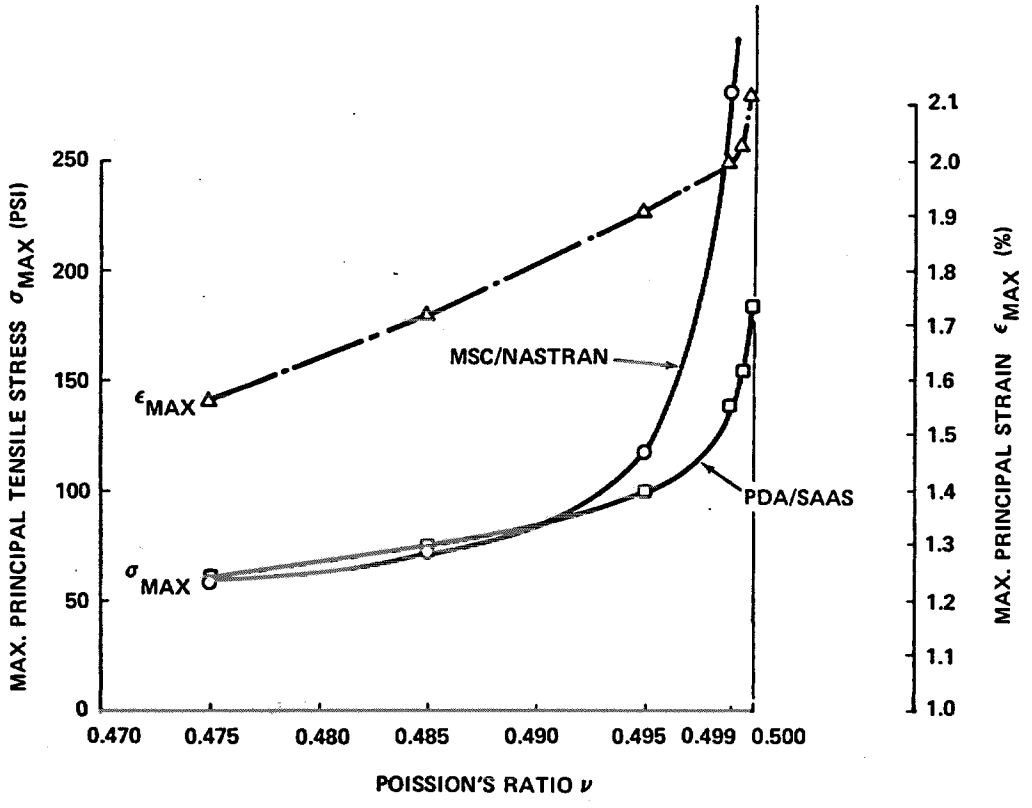

Figure 12. Summary of σ_{max} and ϵ_{max} in Near Incompressibility Study of MSC/NASTRAN Versus PDA/SAAS Using Plane Strain Model of Potting Near Copper Wire (ΔT = -38°C)

CONCLUSIONS

The electrical and thermostructural analysis results indicate that adequate margins exist in the TWT gun design. However, they also point out that finite element analysis capabilities have outpaced the material property base, and more time- and temperature-dependent properties are sorely needed. Development of a combined electrical/mechanical failure criterion is recommended. In the design of potted high-voltage devices such as TWTs, finite element analysis should be performed early in the design phase to detect high stresses in constrained areas and likely locations for electrical breakdown. The analysis will lead to better designs, more optimum use of materials, weight savings, and increased reliability.

ACKNOWLEDGMENT

This work was performed in 1981 for Hughes Aircraft Company, Electron Dynamics Division, Torrance, California under P.O. P3-841005-U08. The authors would like to thank Mr. H. A. Silverman, Program Manager, who provided technical guidance during the study.

REFERENCES

1. Brauer, J. R., "Three-Dimensional Electrostatic Fields of a High Voltage Transmission Line," Proc. Conference on Finite Element Methods and Technology, Pasadena, California, March 1981.

2. Brauer, J. R., "Finite Element Analysis of Electric and Magnetic Fields," First Chautauqua on Finite Element Modeling (ed. J. H. Conaway), Harwichport, Massachusetts, 15-17 September 1980, sponsored by Schaefer Analysis, Inc.

3. Chari, M. V. K. and P. P. Silvester (eds.), Finite Element in Electrical and Magnetic Field Problems, Wiley & Sons (U.K.), 1980.

4. Read, W. S., "Electronic Equipment and Cabling Design and Fabrication Requirements and Processing Techniques - Volume I Design," Jet Propulsion Laboratory, Design Requirement DM 509306 (Rev. C), 1 September 1978, Pasadena, California, pp. 136-138.

5. Fong, H. H. and D. J. Hamel, "Thermal/Structural Analysis of Traveling Wave Tubes Using Finite Elements," IEEE International Electron Devices Meeting, Washington, D. C., 3-5 December 1979, Technical Digest, pp. 295-298.

6. Fong, H. H., "Finite Element Analysis of Traveling Wave Tubes," Finite Element News, September 1980, pp. 26-29.

7. Vichnin, H. H. and H. H. Fong, "Thermostructural Analysis of Potting Compounds in Traveling Wave Tubes and High Voltage Power Supplies," Proc. IEEE National Aerospace and Electronics Conference (NAECON 1981), 19-21 May 1981, Dayton, Ohio., Vol. 2, pp. 454-461.

8. Herrmann, L. R., "Elasticity Equations for Incompressible and Nearly Incompressible Materials by A Variational Theorem," J. AIAA, Vol. 3, No. 10, October 1965, pp. 1896-1900.

9. Nagtegaal, J. C., D. M. Parks and J. R. Rice, "On Numerically Accurate Finite Element Solutions in the Fully Plastic Range," Computer Methods in Applied Mechanics and Engineering, Vol. 4, 1974, pp. 153-177.

10. Malkus, D. S., "A Finite Element Displacement Model Valid for Any Value of the Incompressibility," Int. J. Solids Structures, Vol. 12, 1976, pp. 731-738.

11. Hughes, T. J. R., "Equivalence of Finite Elements for Nearly Incompressible Elasticity," J. of Applied Mechanics, Trans. ASME, Vol. 44, March 1977, pp. 181-183.

12. Malkus, D. S. and T. J. R. Hughes, "Mixed Finite Element Methods-Reduced and Selective Integration Techniques: A Unification of Concepts," Computer Methods in Applied Mechanics and Engineering, Vol. 15, No. 1, July 1978, pp. 63-81.

13. Webster, R. L., "On The Implementation of Incompressibility and Near Incompressibility in Finite Element Solid Mechanics Codes," First Chautauqua on Finite Element Modeling, (ed. J. H. Conaway), Harwichport, Massachusetts, 15-17 September 1980, sponsored by Schaefer Analysis, Inc.

14. Hughes, T. J. R., "Some Current Trends in Finite Element Research," Applied Mechanics Reviews, Vol. 33, No. 11, November 1980, pp. 1467-1477.

15. "The Analysis of Nearly Incompressible Materials," MSC/NASTRAN Application Manual, Section 5, April 1980, pp. 1-19.

16. Fong, H. H., "An Evaluation of Eight U.S. General Purpose Finite-Element Computer Programs," Paper 82-0699-CP to be presented at the 23rd AIAA/ASME/ASCE/AHS Structures, Structural Dynamics and Materials Conference, 10-12 May 1982, New Orleans, Louisiana.

17. Fong, H. H. and J. W. Jones, "An Evaluation of COSMIC/NASTRAN," Presented at the Third World Congress and Exhibition on Finite Element Methods, Beverly Hills, California, 12-16 October 1981. [New and Future Developments in Commercial Finite Element Methods, (ed. J. Robinson), Robinson and Associates, 1981, pp. 324-338.]

18. Crose, J. G. and R. M. Jones, "SAAS III - Finite Element Stress Analysis of Axisymmetric and Plane Solids with Different Orthotropic, Temperature-Dependent Material Properties in Tension and Compression, The Aerospace Corporation, Report No. TR-0059(S6816-53)-1, 22 June 1971.